The Deubiquitinase USP36 Regulates Growth and Spermatogenesis Through Catalytic-Dependent and -Independent Mechanisms in *Drosophila*

Carmen Coirry[1], Julie Manessier[1], Charlène Clot[1, #a], Magda Mortier[1], Marie-Odile Fauvarque[1] and Emmanuel Taillebourg[1, *]

1 Univ. Grenoble Alpes, CEA, INSERM, BGE U1038, F-38000 Grenoble, France

#a Current Address: Institut de Génétique Moléculaire de Montpellier, Univ Montpellier, CNRS, Montpellier, France

* Corresponding author
E-mail: emmanuel.taillebourg@cea.fr

Running title: Catalytic-Dependent and -Independent functions of USP36

Keywords: DUB, MYC, CRISPR/Cas9, cell growth, spermatogenesis

ABSTRACT

Deubiquitinases (DUBs) form a specific class of proteases removing ubiquitin from target proteins. They are involved in the regulation of many cellular processes including cell growth and proliferation. Among them, USP36 is a key regulator of the oncogenic transcription factor c-Myc, preventing its degradation by the proteasome. These two proteins form an evolutionary conserved complex providing the opportunity to investigate USP36 mechanisms of action *in vivo* in a genetically tractable model such as *Drosophila melanogaster*. Null mutants of *dUsp36* die early during larval development and exhibit severe growth defects. Strikingly, we report here that flies carrying a CRISPR/Cas9-induced catalytic mutation of *dUsp36* survive to adulthood with only minor growth defects, yet males are infertile. This finding indicates that dUSP36 deubiquitinating activity is dispensable for cell growth but essential for spermatogenesis. Our results thus reveal that dUSP36 functions through both catalytic-dependent and catalytic-independent mechanisms, highlighting a dual mode of action with implications for the understanding of DUBs mechanism of action.

INTRODUCTION

Deubiquitinases (DUBs) are proteases that specifically remove ubiquitin moieties from ubiquitinated proteins. They regulate numerous cellular processes (Komander et al. 2009; Clague et al. 2013; Leznicki and Kulathu 2017) and their dysregulation has been linked to numerous human cancers (Sacco et al. 2010; Fraile et al. 2018; Dewson et al. 2023). In particular, USP36, a DUB primarily localized in the nucleolus, supports ribosomal biogenesis and maintains nucleolar integrity by deubiquitinating and stabilizing multiple nucleolar proteins, such as c-MYC, DHX33, SNAIL1, and RNA Pol I (Endo, Kitamura, et al. 2009; Endo, Matsumoto, et al. 2009; Sun, He, et al. 2015; Fraile et al. 2018; van den Heuvel et al. 2021; Qin et al. 2023; Yang et al. 2024). The role of USP36 in c-MYC regulation has been extensively studied (Sun, He, et al. 2015; Sun, Sears, et al. 2015; Liu et al. 2019; Thevenon et al. 2020; Hu and Luo 2024), as precise control of c-MYC levels is critical for normal cell growth and proliferation, while its dysregulation contributes to tumorigenesis (van Riggelen et al. 2010; Miller et al. 2012; Sabo and Amati 2014; Grifoni and Bellosta 2015).

51 We previously showed that in *Drosophila melanogaster*, dUSP36 is essential for cell growth,
52 and stabilizes dMYC (Thevenon et al. 2020). To further investigate the *in vivo* mechanisms of
53 action of dUSP36 and assess the specific role of its DUB activity, we generated a catalytically
54 inactive version of the endogenous dUSP36 protein using CRISPR/Cas9 mutagenesis. Here,
55 we demonstrate that unlike *dUsp36* null mutants, which completely lack dUSP36 protein and
56 exhibit severe growth defects leading to larval lethality, *dUsp36* catalytic mutants display
57 only minor growth defects and develop to adulthood. Interestingly, *dUsp36* catalytic mutant
58 males exhibit severely reduced fertility.
59 Altogether, these findings reveal that while the presence of the dUSP36 protein is essential
60 for cellular growth, its catalytic activity is dispensable for this process but critically required
61 for spermatogenesis. These results demonstrate that*, in vivo*, dUSP36 functions through
62 both catalytic-dependent and catalytic-independent mechanisms, revealing a dual mode of
63 action.
64
65
66 RESULTS
67
68 **Generation of *dUsp36* catalytic mutants by CRISPR/Cas9 mutagenesis**
69 To generate a catalytically inactive version of the dUSP36 protein, we mutated the cysteine
70 residue (C181) within a conserved domain previously shown to be essential for DUB catalytic
71 activity (Hu et al. 2005; Komander et al. 2009; Faesen et al. 2011; Ye et al. 2011) to a serine
72 residue (Fig. S1A; see Materials and Methods for details). This C181S mutation has been
73 previously demonstrated to completely abolish dUSP36 catalytic activity (Buszczak et al.
74 2009). The CRISPR/Cas9 mutagenesis yielded two independent $dUsp36^{C181S}$ mutant strains,
75 as well as a control strain, $dUsp36^{CTL}$, which contains the same silent mutations introduced
76 for screening purposes as the mutant alleles but lacks the G-to-C transversion encoding the
77 C181S mutation (Fig. S1C).
78 Western blot analysis of dUSP36 expression revealed that the $dUSP36^{C181S}$ protein is
79 detected at lower levels than the wild-type dUSP36 protein, whereas the $dUsp36^{CTL}$ allele
80 produces normal dUSP36 protein levels (Fig. 1A, B). This observation aligns with previous
81 findings indicating that dUSP36 undergoes auto-deubiquitination to regulate its stability
82 (Thevenon et al. 2020). To ensure comparable dUSP36 protein levels across genotypes, we

83 compared *dUsp36*^{C181S} mutants with *dUsp36*^{CTL}/*dUsp36*$^{\Delta 43}$ heterozygous controls (Fig. 1B).
84 Importantly, the subcellular localization of the dUSP36^{C181S} protein remains indistinguishable
85 from that of the wild-type dUSP36 protein (Fig. 1C). These data confirm the successful
86 generation of the catalytically inactive dUsp36^{C181S} mutant allele, providing a valuable tool
87 for investigating the specific role of dUSP36 catalytic activity *in vivo*.
88
89 ***dUsp36* catalytic mutants are viable and exhibit a subtle growth phenotype**
90 We previously reported that *dUsp36*$^{\Delta 43}$ null mutants, which completely lack dUSP36 protein,
91 exhibit severe cell growth defects and early larval lethality (Taillebourg et al. 2012) indicating
92 that the presence of dUSP36 protein is required for cellular and organismal growth. In sharp
93 contrast with these previous findings, we found that *dUsp36*^{C181S} mutants develop to
94 adulthood without lethality (Fig 2A) and exhibit only a minor reduction in body weight (Fig.
95 2B), along with a slight decrease in wing size (Fig. 2C, D).
96 The enzymatic activity of USPs relies on a catalytic triad—a conserved set of three amino
97 acids consisting of a cysteine, a histidine, and an aspartate or asparagine. Histidine-to-
98 aspartate substitutions have also been reported to render the enzyme catalytically inactive
99 (Kovalenko et al. 2003; Hu et al. 2005; Komander et al. 2009). We mutated both the cysteine
100 and histidine residues and generated transgenic flies expressing the dUSP36$^{C181S, H439D}$
101 protein. When ubiquitously expressed in a *dUsp36* null mutant background, this double
102 mutant protein rescues the larval lethality of *dUsp36* null mutants and allows viable adults to
103 emerge (Fig. S2). These results confirm that the catalytic activity of dUSP36 is not essential
104 for cellular growth and organismal viability.
105 To determine whether the observed phenotypes result from cell-autonomous factors, we
106 generated clones of cells homozygous for either the control allele *dUsp36*^{CTL}, the catalytically
107 inactive allele *dUsp36*^{C181S}, or the null allele *dUsp36*$^{\Delta 43}$ (Fig. 2E). This analysis revealed that
108 *dUsp36*^{C181S} mutant cells are significantly smaller than neighboring wild-type cells, although
109 their growth is much less affected than that of null *dUsp36* mutant cells (Fig. 2F). This
110 observation indicates that the subtle growth defect of *dUsp36* catalytic mutants is cell-
111 autonomous.
112 Altogether, these results demonstrate that while the presence of dUSP36 protein is essential
113 for cellular and organismal growth, its catalytic activity plays only a minor, cell-autonomous
114 role in this process.

115

116 **Altering dMYC protein levels in *dUsp36* catalytic mutants**

117 Experimental data obtained in human cellular models (Kovalenko et al. 2003; Hu et al. 2005;
118 Komander et al. 2009) provide compelling evidence that USP36 depletion affects the stability
119 of nucleolar c-MYC and inhibits cell proliferation. To test whether the minor growth defects
120 of *dUsp36* catalytic mutants depend on dMYC function, we evaluated the phenotypic
121 consequences of altered dMYC protein levels in *dUsp36* wild-type or mutant contexts.
122 To increase dMYC levels, we introduced a transgene expressing a GFP-tagged version of
123 dMYC within its genomic environment, providing additional *dMyc* copies alongside the wild-
124 type *dMyc* locus (Greer et al. 2013). This transgene fully rescues the lethality of $dMyc^{4}$ null
125 mutants, demonstrating that it expresses physiological levels of functional dMYC protein
126 (data not shown). Remarkably, this transgene significantly enhances the body weight of
127 control flies but not that of *dUsp36* catalytic mutants (Fig. 3A). These results indicate that
128 while control flies respond to dMYC overexpression, *dUsp36* catalytic mutants do not.
129 To further explore the genetic interaction between *dMyc* and *dUsp36*, we used the $dMyc^{P0}$
130 hypomorphic mutation that decreases dMYC protein levels and leads to reduced body
131 weight (Johnston et al. 1999). *dUsp36* catalytic mutants and $dMyc^{P0}$ mutants develop to
132 adulthood without lethality (Fig. 3B). In contrast, in a $dMyc^{P0}$ genetic background, the
133 frequency of $dUsp36^{C181S}$ mutants is significantly reduced (Fig. 3B), whereas no such
134 reduction of viability is observed in *dUsp36* control flies. This implies that while dUSP36
135 catalytic activity is dispensable under normal conditions, it becomes critical when *dMyc*
136 function is compromised.
137 To determine whether these findings hold true at the organ level, we compared the effects
138 of altered dMYC protein levels in the developing wing between control flies and *dUsp36*
139 catalytic mutants (Fig. 3C). In this setup, wing-specific increases of dMYC protein levels were
140 achieved by reducing AGO protein levels using a specific RNAi transgene targeting *Ago*.
141 Indeed, AGO is the F-box component of the SCF E3 ligase complex, which ubiquitinates
142 dMYC and negatively regulates its protein levels *in vivo*. Knocking down *Ago* leads to
143 elevated dMYC protein levels and increased tissue growth (Moberg et al. 2004). As expected,
144 in control flies, reducing AGO protein levels results in increased wing area (Fig. 3C). In
145 contrast, in the developing wing of *dUsp36* catalytic mutants, it does not significantly

146 increase wing size (Fig. 3C). These results indicate that increased dMYC levels promote wing
147 growth in control flies but not in *dUsp36* catalytic mutant flies.
148 Conversely, dMYC protein levels were specifically reduced by expressing a *dMyc* targeting
149 RNAi transgene in the developing wing. In that context, both control flies and *dUsp36*
150 catalytic mutants displayed reduced wing size (Fig. 3C). A two-way ANOVA analysis reveals
151 that *dUsp36* catalytic mutants are more affected by dMYC depletion than control flies (Fig.
152 3D).
153 Altogether these results show that increased dMYC levels fail to increase body weight or
154 wing area in *dUsp36* catalytic mutants, whereas they do in control flies. This suggests that
155 reduced dMYC protein levels are not the primary cause of the growth defect of *dUsp36*
156 catalytic mutants. In contrast, *dUsp36* catalytic mutants exhibit a strong sensitivity to dMYC
157 depletion, suggesting that, *in vivo*, dUSP36 catalytic activity acts in the same pathway as
158 dMYC to promote growth.
159
160 ***dUsp36* catalytic mutation affects male fertility**
161 Specific combinations of viable *dUsp36* loss-of-function alleles have been shown to affect
162 male and female fertility (Buszczak et al. 2009). Here, we observed here that $dUsp36^{C181S}$
163 females are slightly, but significantly, less fertile than control females (Fig. 4A). It remains
164 unclear however whether this decreased fertility is due to a general effect related to their
165 reduced body weight or a specific role of dUSP36 catalytic activity in female gametogenesis.
166 Strikingly, *dUsp36* catalytic mutant males produce significantly fewer offspring than control
167 males, with most being completely sterile (Fig. 4B). Consistent with this observation,
168 $dUsp36^{C181S}$ males exhibit reduced seminal vesicle size, indicating lower sperm production
169 compared to controls. Moreover, we show here that dUSP36 protein is widely expressed
170 during spermatogenesis (Fig. 4C, D). These findings reveal that dUSP36 catalytic activity plays
171 a critical role in spermatogenesis.
172
173
174 DISCUSSION
175
176 The data presented here demonstrate that inactivating the catalytic activity of the DUB
177 USP36 in *Drosophila* is not equivalent to its complete or partial depletion. In particular, the

178 catalytic mutant does not display the cellular and organismal growth defects observed in null
179 *dUsp36* mutant. This indicates that dUSP36 functions primarily through non-catalytic
180 mechanisms in these processes. In contrast we report that USP36 DUB activity is essential
181 for male fertility, making it the only process identified so far that strictly depends on USP36
182 enzymatic function.
183 It is unlikely that the *dUsp36*^{C181S} mutation fails to fully inhibit the DUB activity *in vivo*.
184 Indeed, the lower protein levels of dUSP36^{C181S} compared to wild-type dUSP36 (Fig. 1A, B)
185 indicate that it fails to stabilize itself, unlike the wild-type form which undergoes auto-
186 deubiquitination, strongly suggesting that this protein is indeed catalytically inactive
187 (Thevenon et al. 2020). Furthermore, a double-mutant dUSP36 protein, in which both the
188 catalytic cysteine and the histidine residue of the conserved catalytic triad are mutated, is
189 still able to sustain cell and organismal growth in a null mutant background *in vivo*. These
190 results strongly argue against the hypothesis that the minor growth defect observed in
191 dUsp36^{C181S} mutants is due to residual DUB activity.
192 We further demonstrate that *dUsp36* catalytic mutants do not respond to increased dMYC
193 levels. This suggests that reduced dMYC levels do not contribute to the minor growth defects
194 observed in *dUsp36*^{C181S} mutants. However, these mutants are highly sensitive to dMYC
195 depletion, indicating that dUSP36 catalytic activity likely plays a role in the same pathway as
196 dMYC. Taken together, our results indicate that dUSP36 primarily functions independently of
197 its enzymatic activity in promoting cell growth and that – in contrast with previous reports -
198 its catalytic activity is not required for dMYC *stabilization in vivo*.
199 These results should be considered in the context of existing literature, including our own
200 work, showing that in *Drosophila* and human cultured cells, USP36 deubiquitinates and
201 stabilizes MYC (Sun, Sears, et al. 2015; Sun, He, et al. 2015; Thevenon et al. 2020). Several
202 hypotheses could explain this discrepancy: (1) The deubiquitination and stabilization of MYC
203 by USP36 observed in cultured cells may also occur *in vivo* but could be compensated for by
204 redundant regulatory mechanisms. If this is the case, USP36 would be expected to regulate
205 another dMYC-independent growth process through a non-catalytic mechanism. Along these
206 lines, recent studies in human cells indicate that USP36 functions as a SUMO ligase to
207 promote the SUMOylation of specific nucleolar proteins involved in ribosome biogenesis, a
208 process that is crucial for cell and organism growth (Ryu et al. 2021; Chen et al. 2023; Li et al.
209 2023; Li et al. 2024; Yang et al. 2024). In human cells, the catalytic cysteine of USP36 is

210 essential for both its DUB and SUMO ligase activities (Ryu et al. 2021). If *Drosophila* dUSP36
211 functions similarly as its human orthologue, *dUsp36*^{C181S} mutants should also lack SUMO
212 ligase activity, which would impair ribosome biogenesis and induce severe growth defects
213 similar to those observed in *Minute* mutants (Marygold et al. 2007). However, the mild growth
214 phenotype of *dUsp36*^{C181S} mutants does not support this hypothesis. Additionally, we failed
215 to detect SUMO ligase activity for dUSP36 in *Drosophila* cells (data not shown). (2) Contrary
216 to previous conclusions based on knock-down experiments, USP36 may control MYC stability
217 independently of its catalytic activity: it may not directly deubiquitinate MYC but instead
218 regulate its ubiquitination level indirectly. This could occur through inhibition of an E3 ligase
219 targeting MYC or recruitment of another DUB within the regulatory complex. In this model,
220 USP36 knock-down via RNAi or loss-of-function mutations would impair these functions,
221 leading to MYC destabilization. Moreover, overexpressing wild-type USP36 may result in
222 non-specific deubiquitination of MYC, whereas a catalytically inactive USP36 mutant would
223 not act ectopically, falsely leading to the conclusion that USP36 directly deubiquitinates MYC
224 (Sun, He, et al. 2015; Thevenon et al. 2020). Additional experiments will be needed to clarify
225 the exact mechanisms by which USP36 regulates MYC and contributes to cell growth.
226 While dUSP36 catalytic activity plays a minor role in cell and organismal growth, our results
227 clearly demonstrate that it is essential for spermatogenesis. This is consistent with previous
228 findings showing that dUSP36 is required for germline stem cell maintenance by
229 deubiquitinating histone H2B and repressing premature expression of differentiation genes
230 (Buszczak et al. 2009).
231 In conclusion, our findings indicate that, in *Drosophila*, dUSP36 functions through a dual
232 mechanism: in cell growth, dUSP36 acts independently of its catalytic activity, similar to
233 other DUBs or pseudo-DUBs (Campos Alonso and Knobeloch 2024) whereas in
234 spermatogenesis, its DUB activity is crucial, highlighting a specialized catalytic function in
235 germline development. Our results therefore reshape our understanding of how DUBs
236 functions during cellular responses and development, extending beyond their enzymatic
237 activity. Determining whether this dual mechanism is unique to dUSP36 or extends to its
238 human counterpart and other DUBs will be of great interest.
239
240
241 MATERIALS AND METHODS

242

243 **Drosophila strains**

244 The Bloomington Drosophila Stock Center provided the following Drosophila strains: *Tg*
245 *dMyc* (#81274), *dMyc*^{P0} (#11298), *UAS-dMyc-IR* (# 25783), *UAS-Ago-IR* (#34802), *nubGal4*
246 (#25754), *hsFLP* (#8862), *FRT2A Gal80* (#5190), *FRT2A* (#1997) and *CgGal4* (#7011).

247

248 **CRISPR/Cas9 mutagenesis**

249 The gRNA sequence was selected using the E-CRISP website and cloned into the pCFD3
250 plasmid (Port et al. 2014). A 169-nucleotide long single stranded oligonucleotide donor
251 (ssODN) repair template was synthesised (https://eu.idtdna.com/page). It contains the
252 mutation of interest, a silent mutation creatin g a Pst1 restriction site as well as silent
253 mutations in the PAM and the gRNA to avoid re-cleaving of an edited chromosome (Sup. Fig.
254 1A). The ssODN was injected along with the sgRNA expression vector (ssODN: 100 ng/uL and
255 sgRNA: 250 ng/uL) into the *nos-Cas9* (Port et al. 2014) recipient strain (BestGene Inc.). Sixty-
256 six F0 founders were crossed individually and up to 10 F1 males were crossed individually for
257 each F0 founder; each F1 male was then retrieved for single fly PCR. After amplification, PCR
258 products were digested by Pst1, leading to the identification of six independent Pst1 positive
259 strains (Sup. Fig. 1B). Sequencing revealed that three of them contained the desired C181S
260 mutation (two, *dUsp36*$^{C181S-1}$ and *dUsp36*$^{C181S-2}$, were kept for further analysis) whereas three
261 others did not include the C181S mutation but contains all the silent mutations (Sup. Fig.
262 1C). One of them, *dUsp36*^{CTL}, was used as control.
263 To ensure that the mutagenesis process did not add any off-target mutations, the genomic
264 region was sequenced and these alleles were outcrossed for six generations on a wild-type
265 chromosome. Moreover, all the phenotypic analyses were performed on heterozygotes
266 (*dUsp36*^{CTL}/*dUsp36*$^{\Delta 43}$ and *dUsp36*$^{C181S-1}$/*dUsp36*$^{C181S-2}$).

267

268 **Western blots**

269 Protein lysates were separated on SDS-PAGE gels (TGX Stain Free, BioRad). Proteins were
270 transferred to PVDF membranes (BioRad) which were treated as already described
271 (Thevenon et al. 2020). Image acquisitions were performed with the Chemidoc imaging
272 system (BioRad) and quantifications using the Image Lab software (BioRad). The anti-dUSP36
273 antibody, a kind gift from Dr. M. Buszczak, was used at a 1/2500 dilution

274

275 **Immunohistochemistry**

276 Lateral lobes of third instar larval fat bodies or adult testes were dissected in PBS, fixed for
277 30 min in 4% paraformaldehyde and rinsed twice in PBS. The samples were then blocked for
278 1 h in PBS, 0.1% Triton X-100, 5% normal goat serum and incubated overnight at 4°C with the
279 anti-dUSP36 (1/200) and anti-Fibrillarin 38F3 (1/200, abcam) antibodies. Secondary
280 antibodies were coupled to Alexa594 or Alexa488 (1/500, Invitrogen). After mounting in
281 DAPI containing Vectashield (Vector Laboratories, H-1200), the samples were imaged using a
282 Zeiss LSM 880 confocal laser scanning microscope.

283

284 **Phenotypic analysis**

285 For weight measurements, the larval density was carefully controlled. Three-day-old females
286 were weighted by groups of ten on a Mettler Toledo Classic precision balance. Adults and
287 dissected wings were imaged using a Keyence VHX-5000 numerical microscope. Wing areas
288 were blindly measured manually using the Fiji/ImageJ software (National Institute of Health).
289 For clonal analysis of cell size in the fat body, 0–6 h embryos were subjected to heat-shock
290 for 1 h at 37°C and resulting 4.5 days old L3 larvae were dissected. Fat body's lateral lobes
291 were fixed for 30 min in 4% paraformaldehyde, rinsed twice in PBS, and incubated overnight
292 at 4°C in 2 U/ml Alexa Fluor 546 Phalloidin (Invitrogen, A22283). After mounting in DAPI
293 containing Vectashield (Vector Laboratories, H-1200), the samples were imaged using a Zeiss
294 LSM 880 confocal laser scanning microscope. Cell size was quantified using the Fiji/ImageJ
295 software (National Institute of Health) as the ratio between the area of a GFP+ cell and the
296 mean area of neighbouring GFP- cells.
297 For fertility tests, female and male flies of the indicated genotype were collected, aged for
298 3 days, and individually mated to wild-type flies. The vials were emptied after a three-day
299 period and the progeny was counted.
300 Statistical analyses were performed using the GraphPad Prism6 software.

301

302

303 AKNOWLEDGEMENT

304

305 We thank Dr. Buszczak for the anti-dUSP36 antibody, the Bloomington *Drosophila* Stock
306 Center for providing *Drosophila* strains, and the IRIG µLife facility for confocal microscopy.
307 This work was supported by the French National Research Agency in the framework of the
308 "Investissements d'avenir" program (ANR-17-EURE-0003) through a funding from GRAL.
309 Thesis operating costs are supported by IDEX Université Grenoble Alpes and GRAL PhD
310 Operating Costs (CC).

311

312

313 REFERENCES

314

315 Buszczak M, Paterno S, Spradling AC. 2009. Drosophila stem cells share a common
316 requirement for the histone H2B ubiquitin protease scrawny. Science. 323(5911):248–51.
317 doi:10.1126/science.1165678.

318 Campos Alonso M, Knobeloch KP. 2024. In the moonlight: non-catalytic functions of
319 ubiquitin and ubiquitin-like proteases. Front Mol Biosci. 11:1349509.
320 doi:10.3389/fmolb.2024.1349509.

321 Chen Y, Li Y, Dai RS, Savage JC, Shinde U, Klimek J, David LL, Young EA, Hafner M, Sears RC, et
322 al. 2023. The ubiquitin-specific protease USP36 SUMOylates EXOSC10 and promotes the
323 nucleolar RNA exosome function in rRNA processing. Nucleic Acids Res. 51(8):3934–3949.
324 doi:10.1093/nar/gkad140.

325 Clague MJ, Barsukov I, Coulson JM, Liu H, Rigden DJ, Urbe S. 2013. Deubiquitylases from
326 genes to organism. Physiol Rev. 93(3):1289–315. doi:10.1152/physrev.00002.2013.

327 Dewson G, Eichhorn PJA, Komander D. 2023. Deubiquitinases in cancer. Nat Rev Cancer.
328 23(12):842–862. doi:10.1038/s41568-023-00633-y.

329 Endo A, Kitamura N, Komada M. 2009. Nucleophosmin/B23 regulates ubiquitin dynamics in
330 nucleoli by recruiting deubiquitylating enzyme USP36. J Biol Chem. 284(41):27918–27923.
331 doi:10.1074/jbc.M109.037218.

332 Endo A, Matsumoto M, Inada T, Yamamoto A, Nakayama KI, Kitamura N, Komada M. 2009.
333 Nucleolar structure and function are regulated by the deubiquitylating enzyme USP36. J Cell
334 Sci. 122(Pt 5):678–86. doi:10.1242/jcs.044461.

335 Faesen AC, Luna-Vargas MP, Geurink PP, Clerici M, Merkx R, van Dijk WJ, Hameed DS, El
336 Oualid F, Ovaa H, Sixma TK. 2011. The differential modulation of USP activity by internal
337 regulatory domains, interactors and eight ubiquitin chain types. Chem Biol. 18(12):1550–61.
338 doi:10.1016/j.chembiol.2011.10.017.

339 Fraile JM, Campos-Iglesias D, Rodriguez F, Astudillo A, Vilarrasa-Blasi R, Verdaguer-Dot N,
340 Prado MA, Paulo JA, Gygi SP, Martin-Subero JI, et al. 2018. Loss of the deubiquitinase USP36

341 destabilizes the RNA helicase DHX33 and causes preimplantation lethality in mice. J Biol
342 Chem. 293(6):2183–2194. doi:10.1074/jbc.M117.788430.

343 Greer C, Lee M, Westerhof M, Milholland B, Spokony R, Vijg J, Secombe J. 2013. Myc-
344 dependent genome instability and lifespan in Drosophila. PLoS One. 8(9):e74641.
345 doi:10.1371/journal.pone.0074641.

346 Grifoni D, Bellosta P. 2015. Drosophila Myc: A master regulator of cellular performance.
347 Biochim Biophys Acta. 1849(5):570–81. doi:10.1016/j.bbagrm.2014.06.021.

348 van den Heuvel J, Ashiono C, Gillet LC, Dorner K, Wyler E, Zemp I, Kutay U. 2021. Processing
349 of the ribosomal ubiquitin-like fusion protein FUBI-eS30/FAU is required for 40S maturation
350 and depends on USP36. Elife. 10. doi:10.7554/eLife.70560.

351 Hu M, Li P, Song L, Jeffrey PD, Chenova TA, Wilkinson KD, Cohen RE, Shi Y. 2005. Structure
352 and mechanisms of the proteasome-associated deubiquitinating enzyme USP14. EMBO J.
353 24(21):3747–56. doi:10.1038/sj.emboj.7600832.

354 Hu Y, Luo M. 2024. Cinobufotalin regulates the USP36/c-Myc axis to suppress malignant
355 phenotypes of colon cancer cells in vitro and in vivo. Aging (Albany NY). 16(6):5526–5544.
356 doi:10.18632/aging.205661.

357 Johnston LA, Prober DA, Edgar BA, Eisenman RN, Gallant P. 1999. Drosophila myc regulates
358 cellular growth during development. Cell. 98(6):779–90.

359 Komander D, Clague MJ, Urbe S. 2009. Breaking the chains: structure and function of the
360 deubiquitinases. Nat Rev Mol Cell Biol. 10(8):550–63. doi:10.1038/nrm2731.

361 Kovalenko A, Chable-Bessia C, Cantarella G, Israel A, Wallach D, Courtois G. 2003. The
362 tumour suppressor CYLD negatively regulates NF-kappaB signalling by deubiquitination.
363 Nature. 424(6950):801–5. doi:10.1038/nature01802.

364 Leznicki P, Kulathu Y. 2017. Mechanisms of regulation and diversification of deubiquitylating
365 enzyme function. J Cell Sci. 130(12):1997–2006. doi:10.1242/jcs.201855.

366 Li J, Olson LM, Zhang Z, Li L, Bidder M, Nguyen L, Pfeifer J, Rader JS. 2008. Differential display
367 identifies overexpression of the USP36 gene, encoding a deubiquitinating enzyme, in ovarian
368 cancer. Int J Med Sci. 5(3):133–42. doi:10.7150/ijms.5.133.

369 Li Y, Carey TS, Feng CH, Zhu HM, Sun XX, Dai MS. 2023. The Ubiquitin-specific Protease
370 USP36 Associates with the Microprocessor Complex and Regulates miRNA Biogenesis by
371 SUMOylating DGCR8. Cancer Res Commun. 3(3):459–470. doi:10.1158/2767-9764.CRC-22-
372 0344.

373 Li Y, Yang Y, Sears RC, Dai MS, Sun XX. 2024. USP36 SUMOylates Las1L and Promotes Its
374 Function in Pre-Ribosomal RNA ITS2 Processing. Cancer Res Commun. 4(10):2835–2845.
375 doi:10.1158/2767-9764.CRC-24-0312.

376 Liu Q, Sheng W, Ma Y, Zhen J, Roy S, Alvira Jafar C, Xin W, Wan Q. 2019. USP36 protects
377 proximal tubule cells from ischemic injury by stabilizing c-Myc and SOD2. Biochem Biophys
378 Res Commun. 513(2):502–508. doi:10.1016/j.bbrc.2019.03.043.

379 Luo L, Li Y, Huang R, Li L, Wu C, Zeng Q. 2024. USP36 plays an oncogenic role in colorectal
380 cancer cells. Neoplasma. 71(1):13–21. doi:10.4149/neo_2023_230629N339.

381 Marygold SJ, Roote J, Reuter G, Lambertsson A, Ashburner M, Millburn GH, Harrison PM, Yu
382 Z, Kenmochi N, Kaufman TC, et al. 2007. The ribosomal protein genes and Minute loci of
383 Drosophila melanogaster. Genome Biol. 8(10):R216. doi:10.1186/gb-2007-8-10-r216.

384 Miller DM, Thomas SD, Islam A, Muench D, Sedoris K. 2012. c-Myc and cancer metabolism.
385 Clin Cancer Res. 18(20):5546–53. doi:10.1158/1078-0432.CCR-12-0977.

386 Moberg KH, Mukherjee A, Veraksa A, Artavanis-Tsakonas S, Hariharan IK. 2004. The
387 Drosophila F box protein archipelago regulates dMyc protein levels in vivo. Curr Biol.
388 14(11):965–74. doi:10.1016/j.cub.2004.04.040.

389 Niu MY, Liu YJ, Shi JJ, Chen RY, Zhang S, Li CY, Cao JF, Yang GJ, Chen J. 2024. The Emerging
390 Role of Ubiquitin-Specific Protease 36 (USP36) in Cancer and Beyond. Biomolecules. 14(5).
391 doi:10.3390/biom14050572.

392 Port F, Chen HM, Lee T, Bullock SL. 2014. Optimized CRISPR/Cas tools for efficient germline
393 and somatic genome engineering in Drosophila. Proc Natl Acad Sci U S A. 111(29):E2967-76.
394 doi:10.1073/pnas.1405500111.

395 Qin K, Yu S, Liu Y, Guo R, Guo S, Fei J, Wang Y, Jia K, Xu Z, Chen H, et al. 2023. USP36
396 stabilizes nucleolar Snail1 to promote ribosome biogenesis and cancer cell survival upon
397 ribotoxic stress. Nat Commun. 14(1):6473. doi:10.1038/s41467-023-42257-8.

398 van Riggelen J, Yetil A, Felsher DW. 2010. MYC as a regulator of ribosome biogenesis and
399 protein synthesis. Nat Rev Cancer. 10(4):301–9. doi:10.1038/nrc2819.

400 Ryu H, Sun XX, Chen Y, Li Y, Wang X, Dai RS, Zhu HM, Klimek J, David L, Fedorov LM, et al.
401 2021. The deubiquitinase USP36 promotes snoRNP group SUMOylation and is essential for
402 ribosome biogenesis. EMBO Rep. 22(6):e50684. doi:10.15252/embr.202050684.

403 Sabo A, Amati B. 2014. Genome recognition by MYC. Cold Spring Harb Perspect Med. 4(2).
404 doi:10.1101/cshperspect.a014191.

405 Sacco JJ, Coulson JM, Clague MJ, Urbe S. 2010. Emerging roles of deubiquitinases in cancer-
406 associated pathways. IUBMB Life. 62(2):140–57. doi:10.1002/iub.300.

407 Sun XX, He X, Yin L, Komada M, Sears RC, Dai MS. 2015. The nucleolar ubiquitin-specific
408 protease USP36 deubiquitinates and stabilizes c-Myc. Proc Natl Acad Sci U S A.
409 112(12):3734–9. doi:10.1073/pnas.1411713112.

410 Sun XX, Sears RC, Dai MS. 2015. Deubiquitinating c-Myc: USP36 steps up in the nucleolus.
411 Cell Cycle. 14(24):3786–93. doi:10.1080/15384101.2015.1093713.

412 Taillebourg E, Gregoire I, Viargues P, Jacomin AC, Thevenon D, Faure M, Fauvarque MO.
413 2012. The deubiquitinating enzyme USP36 controls selective autophagy activation by
414 ubiquitinated proteins. Autophagy. 8(5):767–79. doi:10.4161/auto.19381.

415 Thevenon D, Seffouh I, Pillet C, Crespo-Yanez X, Fauvarque MO, Taillebourg E. 2020. A
416 Nucleolar Isoform of the Drosophila Ubiquitin Specific Protease dUSP36 Regulates MYC-
417 Dependent Cell Growth. Front Cell Dev Biol. 8:506. doi:10.3389/fcell.2020.00506.

418 Xu H, Wang T, Nie H, Sun Q, Jin C, Yang S, Chen Z, Wang X, Tang J, Feng Y, et al. 2024. USP36
419 promotes colorectal cancer progression through inhibition of p53 signaling pathway via
420 stabilizing RBM28. Oncogene. 43(47):3442–3455. doi:10.1038/s41388-024-03178-y.

421 Yang Y, Li Y, Sears RC, Sun XX, Dai MS. 2024. SUMOylation regulation of ribosome biogenesis:
422 Emerging roles for USP36. Front RNA Res. 2. doi:10.3389/frnar.2024.1389104.

423 Ye Y, Akutsu M, Reyes-Turcu F, Enchev RI, Wilkinson KD, Komander D. 2011. Polyubiquitin
424 binding and cross-reactivity in the USP domain deubiquitinase USP21. EMBO Rep. 12(4):350–
425 7. doi:10.1038/embor.2011.17.

426 FIGURE LEGENDS

427

428 Figure 1

429 Expression of the dUSP36^{C181S} protein. (A) Total protein extracts from *Drosophila* males of
430 the indicated genotypes were analysed by Western blot using a specific anti-dUSP36
431 antibody. (B) Quantification of dUSP36 relative levels, expressed as the ratio of dUSP36
432 signal intensity to Actin signal intensity, normalized to the wild-type Canton-S strain. N = 4.
433 ** indicates a statistically significant difference (P < 0.01) as determined by one-way ANOVA.
434 (C) Fat bodies of third-instar larvae stained with anti-dUSP36 and anti-Fibrillarin antibodies.
435 Images are shown as separate grayscale channels and as merged images. Blue: DAPI. Green:
436 anti-dUSP36. Red: anti-Fibrillarin.

437

438 Figure 2

439 Phenotype of *dUsp36*^{C181S} mutants. (A) Histograms showing the observed frequency of the
440 indicated genotypes in the progeny resulting from the following crosses: *dUsp36*^{WT} x
441 *dUsp36*$^{\Delta 43}$*/TM6b* ,*dUsp36*^{CTL} x *dUsp36*$^{\Delta 43}$*/TM6b*, and *dUsp36*$^{C181S\text{-}1}$ x *dUsp36*$^{C181S\text{-}2}$*/TM6b*
442 respectively. (B) Weight of groups of ten *Drosophila* females of the indicated genotype. (C)
443 Dissected wings and (D) wing area quantifications. (E) GFP-positive clones of larval fat body
444 cells homozygous for the indicated *dUsp36* allele. (F) Quantifications of the relative cell size,
445 expressed as the ratio between the area of a GFP+ cell and the mean area of neighbouring
446 GFP- cells (F). Genotype: *hsFLP*/+; *CgGal4, UAS-GFP*/+; *FRT2A dUsp36*^{x}*/FRT2A TubGal80*.
447 **** and *** indicate statistical significance with P < 0.001 and P < 0.01, respectively, as
448 determined by chi-square test (A) and one-way ANOVA (B, D, F).

449

450 Figure 3

451 Phenotypic effects of dMYC levels increase and decrease in *dUsp36* catalytic mutants. (A)
452 Quantifications and statistical analyses of female fly weight for the indicated genotypes. "*Tg*
453 *dMyc*" indicates the presence at the homozygous state of a transgene expressing a GFP-
454 tagged version of dMYC within its genomic environment. (B) Histograms showing the
455 observed frequency of males of the indicated genotypes in the progeny resulting from the
456 following crosses: *dUsp36*^{CTL}*/TM6b* x *dUsp36*$^{\Delta 43}$*/TM6b*, *dUsp36*$^{C181S\text{-}1}$*/TM6b* x *dUsp36*$^{C181S\text{-}}$
457 ^{2}*/TM6b*, *dMyc*^{P0}*/FM7c*; *dUsp36*^{CTL}*/TM6b* x *dUsp36*$^{\Delta 43}$*/TM6b*, and *dMyc*^{P0}*/FM7c*; *dUsp36*$^{C181S\text{-}}$

458 ^{1}/*TM6b* x *dUsp36*$^{C181S-2}$/*TM6b*, respectively. (C, D) Quantifications and statistical analyses of
459 wing areas of control and catalytic mutant flies expressing the wing-specific Gal4 driver
460 *nubGal4*, either alone or in combination with RNAi transgenes targeting *dMyc* or *ago*. ****
461 and *** indicate statistical significance with P < 0.001 and P < 0.01, respectively, as
462 determined by one-way ANOVA (A, C), chi-square test (B), and two-way ANOVA (D).
463
464 Figure 4
465 Fertility defects in *dUsp36* catalytic mutants. Quantifications and statistical analyses of the
466 number of offspring produced by individual females (A) and males (B) of the indicated
467 genotypes. (C) Testis stained with anti-dUSP36. The seminal vesicle is outlined. Blue: DAPI.
468 Green: anti-dUSP36 antibody. (D) Quantifications and statistical analyses of the area of the
469 seminal vesicle (S.V.). **** and *** indicate statistical significance with P < 0.001 and P <
470 0.01, respectively, as determined by one-way ANOVA."**
471
472 Figure S1
473 Generation of *dUsp36* catalytic mutants by CRISPR/Cas9 mutagenesis. (A) Schematic
474 representation of the *dUsp36* locus with the three known isoforms. The position of the
475 codon specifying the cysteine residue at position 181 is indicated as well as the gRNA (red
476 triangle). WT: wild-type *dUsp36* sequence showing the targeted cysteine (in cyan), the
477 sequence targeted by the gRNA (underlined in black) and the PAM (underlined in red).
478 ssDNA: part of the ssODN sequence with the G-to-C transversion responsible for the C181S
479 mutation and the silent mutations introduced for screening purposes (creation of a Pst1
480 restriction site and mutation of the PAM and of the gRNA to avoid re-cleaving of an edited
481 chromosome). (B) Agarose gel showing that PCR products amplified from the *dUsp36*^{CTL},
482 *dUsp36*$^{C181S-1}$ and *dUsp36*$^{C181S-2}$ alleles display a Pst1 restriction site which is absent of the
483 wild-type allele. (D) Chromatograms showing the sequences obtained from the two
484 independent *dUsp36*^{C181S} alleles, as well as from the control allele, *dUsp36*^{CTL}, which contains
485 all the silent mutations introduced for screening purposes but not the G-to-C transversion
486 responsible for the C181S mutation.
487
488 Figure S2

489 Rescue of the lethality of *dUsp36* null mutants by the ubiquitous expression of the double

490 mutant dUSP36$^{C181S,\ H439D}$ protein.

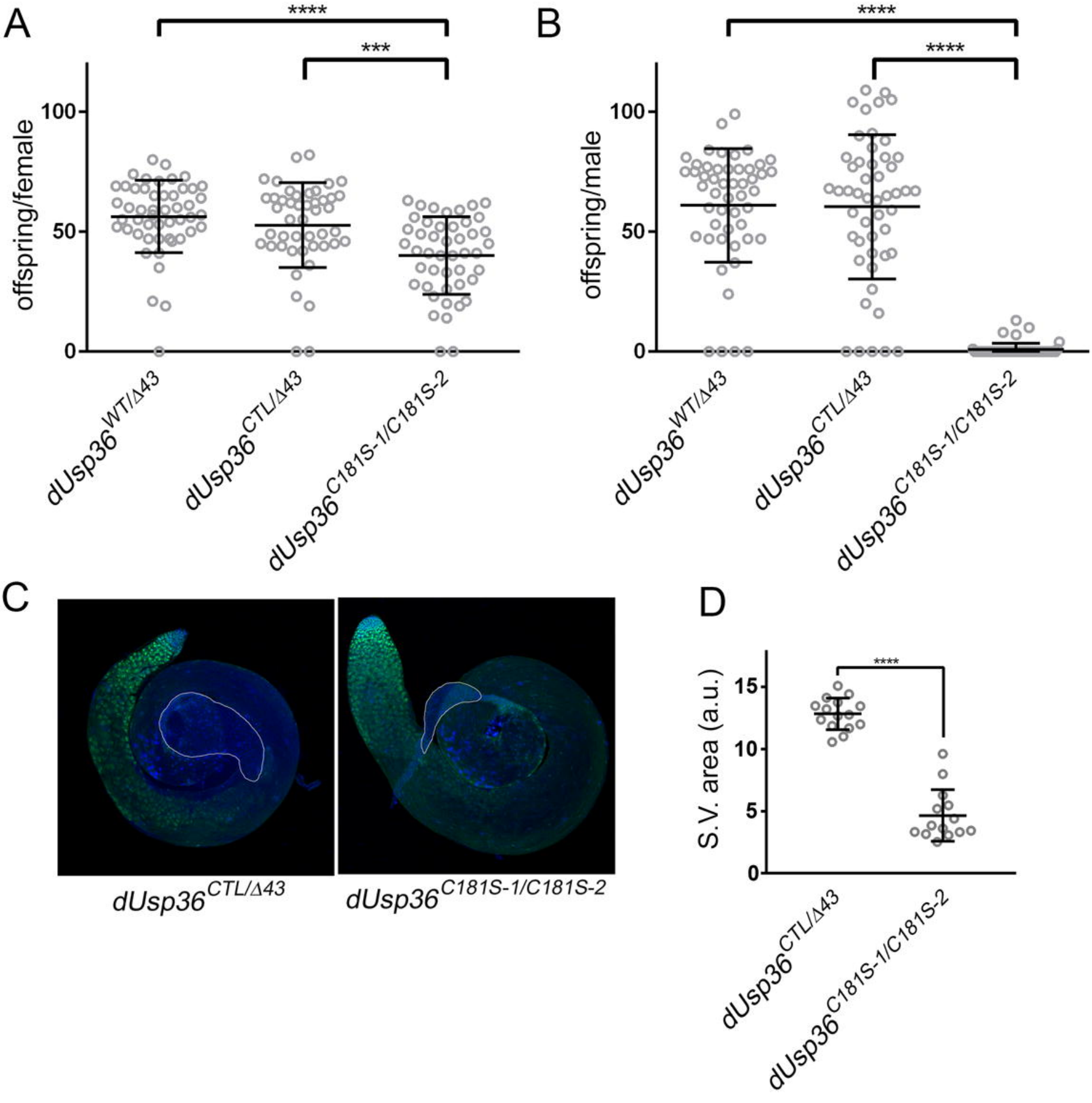
A
****
***
offspring/female
100
50
0
dUsp36WT/Δ43
dUsp36CTL/Δ43
dUsp36C181S-1/C181S-2
B
****
****
offspring/male
100
50
0
dUsp36WT/Δ43
dUsp36CTL/Δ43
dUsp36C181S-1/C181S-2
C
dUsp36CTL/Δ43
dUsp36C181S-1/C181S-2
D
****
S.V. area (a.u.)
15
10
5
0
dUsp36CTL/Δ43
dUsp36C181S-1/C181S-2

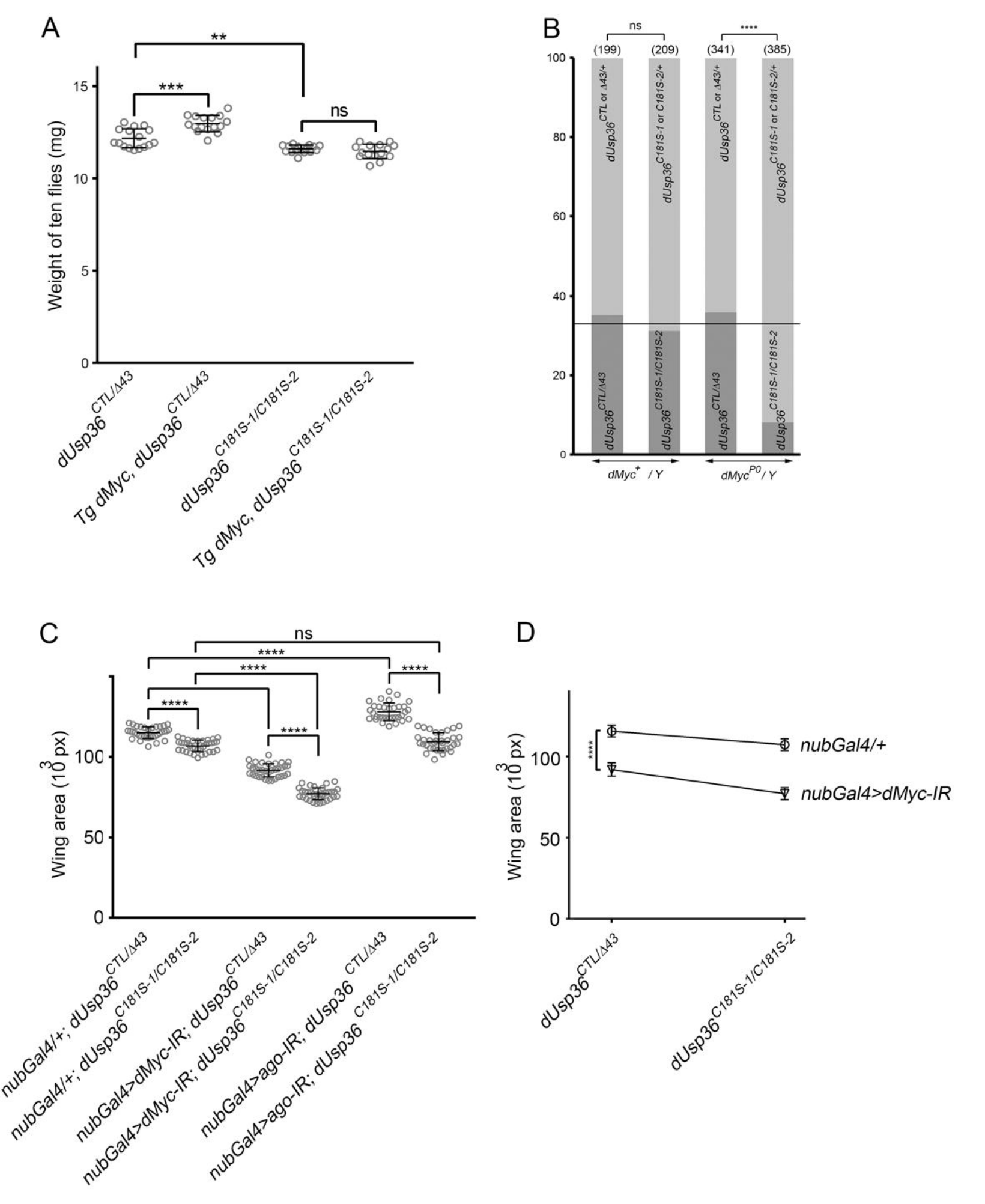
A
Weight of ten flies (mg)
**
***
ns
dUsp36CTL/Δ43
Tg dMyc, dUsp36CTL/Δ43
dUsp36C181S-1/C181S-2
Tg dMyc, dUsp36C181S-1/C181S-2
B
ns
****
(199)
(209)
(341)
(385)
dUsp36CTL or Δ43/+
dUsp36C181S-1 or C181S-2/+
dUsp36CTL/Δ43
dUsp36C181S-1/C181S-2
dMyc+ / Y
dMycP0 / Y
C
Wing area (10^3 px)
ns
****
nubGal4/+; dUsp36CTL/Δ43
nubGal4/+; dUsp36C181S-1/C181S-2
nubGal4>dMyc-IR; dUsp36CTL/Δ43
nubGal4>dMyc-IR; dUsp36C181S-1/C181S-2
nubGal4>ago-IR; dUsp36CTL/Δ43
nubGal4>ago-IR; dUsp36C181S-1/C181S-2
D
Wing area (10^3 px)
nubGal4/+
nubGal4>dMyc-IR
dUsp36CTL/Δ43
dUsp36C181S-1/C181S-2

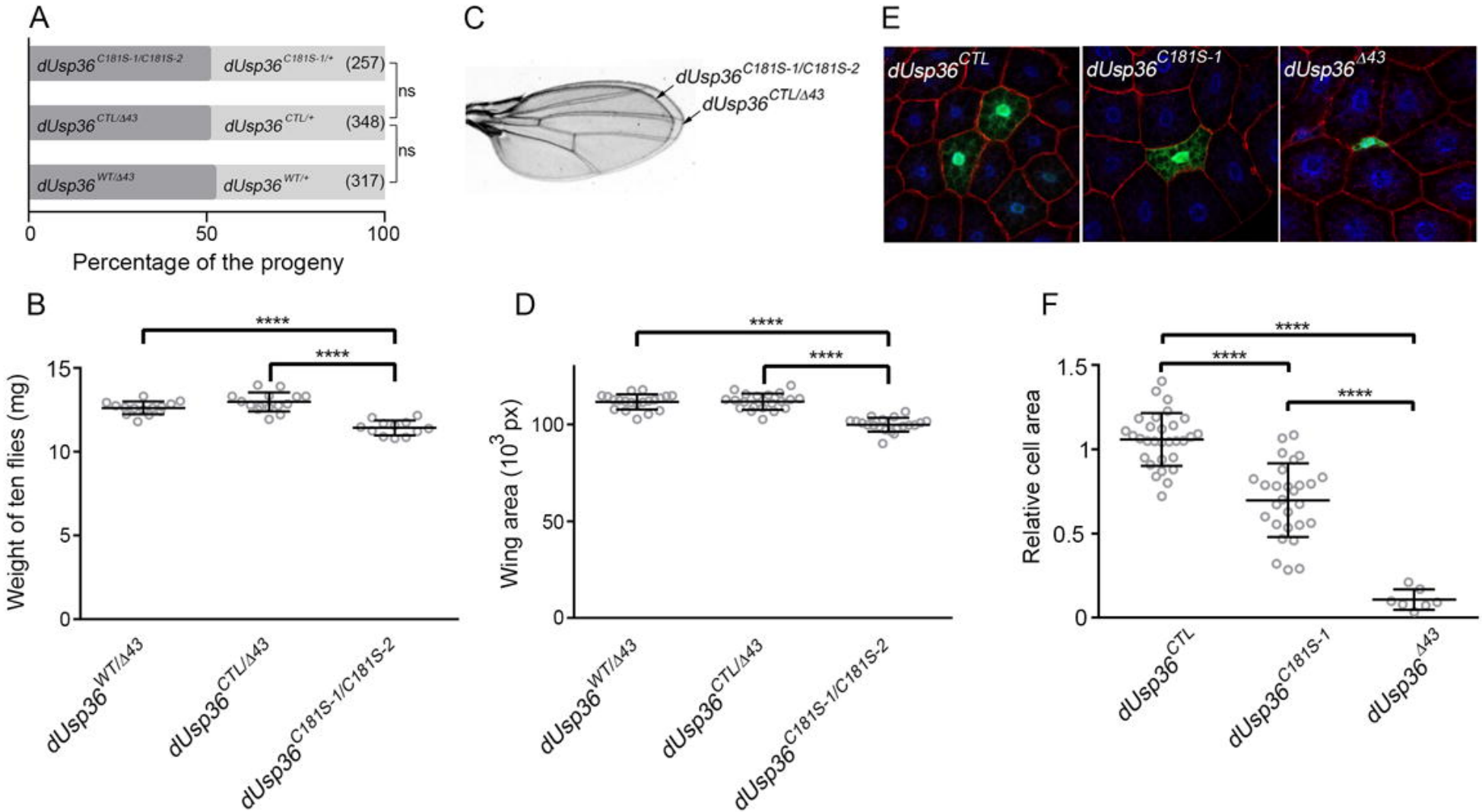
A
dUsp36C181S-1/C181S-2
dUsp36C181S-1/+
(257)
ns
dUsp36CTL/Δ43
dUsp36CTL/+
(348)
ns
dUsp36WT/Δ43
dUsp36WT/+
(317)
0
50
100
Percentage of the progeny
C
dUsp36C181S-1/C181S-2
dUsp36CTL/Δ43
E
dUsp36CTL
dUsp36C181S-1
dUsp36Δ43
B
****
****
Weight of ten flies (mg)
15
10
5
0
dUsp36WT/Δ43
dUsp36CTL/Δ43
dUsp36C181S-1/C181S-2
D
****
****
Wing area (10^3 px)
100
50
0
dUsp36WT/Δ43
dUsp36CTL/Δ43
dUsp36C181S-1/C181S-2
F
****
****
****
Relative cell area
1.5
1
0.5
0
dUsp36CTL
dUsp36C181S-1
dUsp36Δ43

A

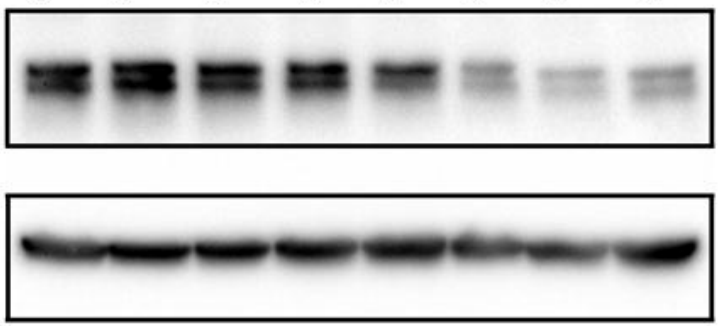
Canton-S
dUsp36WT
dUsp36CTL
dUsp36WT/Δ43
dUsp36CTL/Δ43
dUsp36C181S-1/C181S-2
dUsp36C181S-1
dUsp36C181S-2
dUSP36
Actin

B

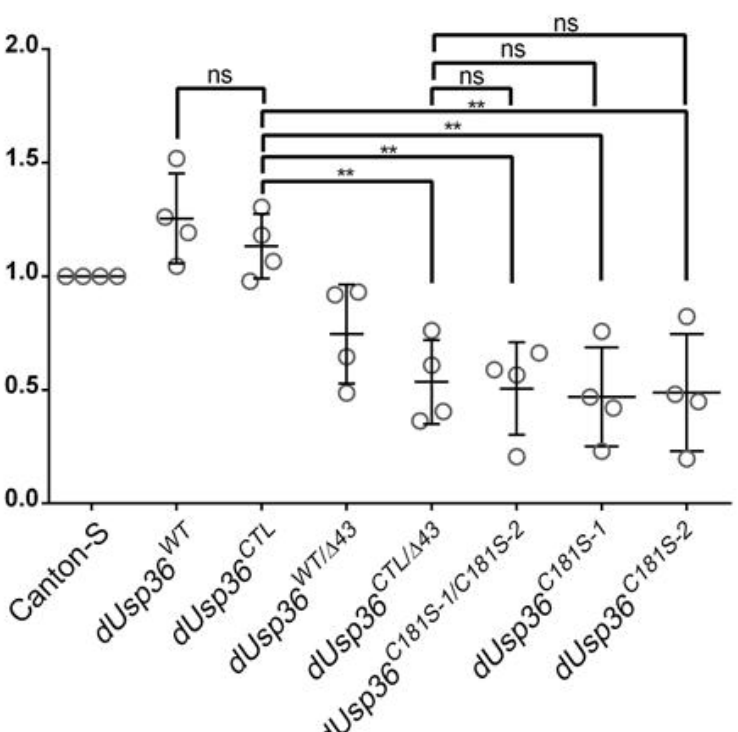
2.0
1.5
1.0
0.5
0.0
ns
ns
ns
ns
**
**
**
**
Canton-S
dUsp36WT
dUsp36CTL
dUsp36WT/Δ43
dUsp36CTL/Δ43
dUsp36C181S-1/C181S-2
dUsp36C181S-1
dUsp36C181S-2

C

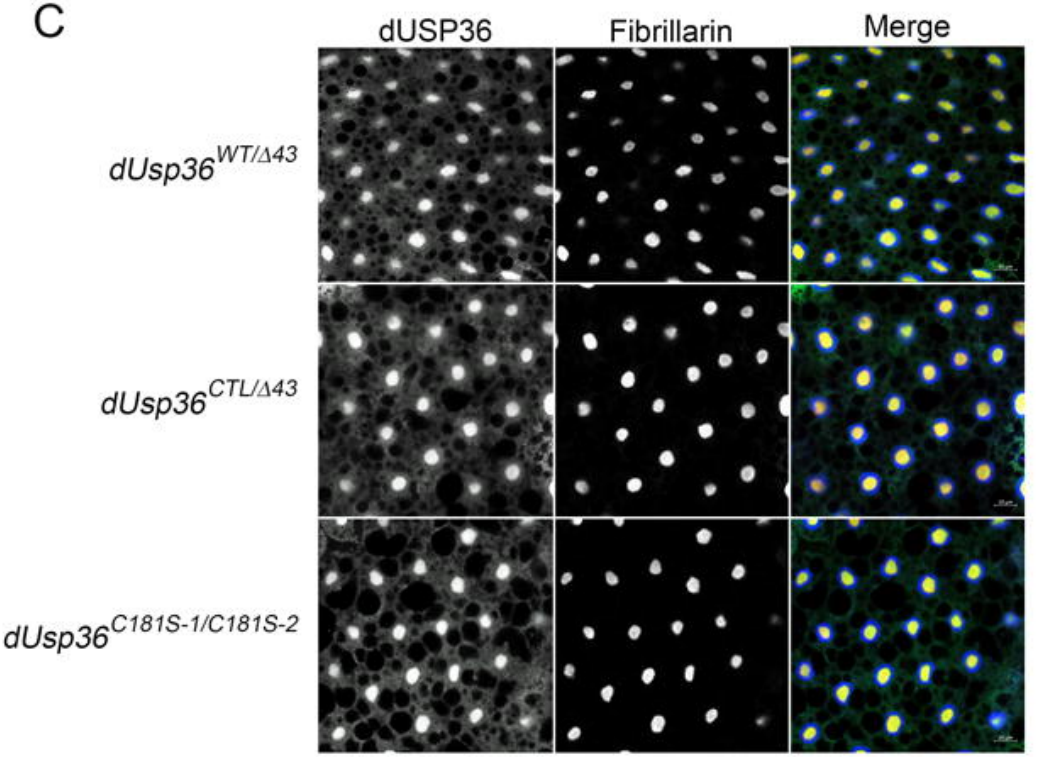
dUSP36
Fibrillarin
Merge
dUsp36WT/Δ43
dUsp36CTL/Δ43
dUsp36C181S-1/C181S-2

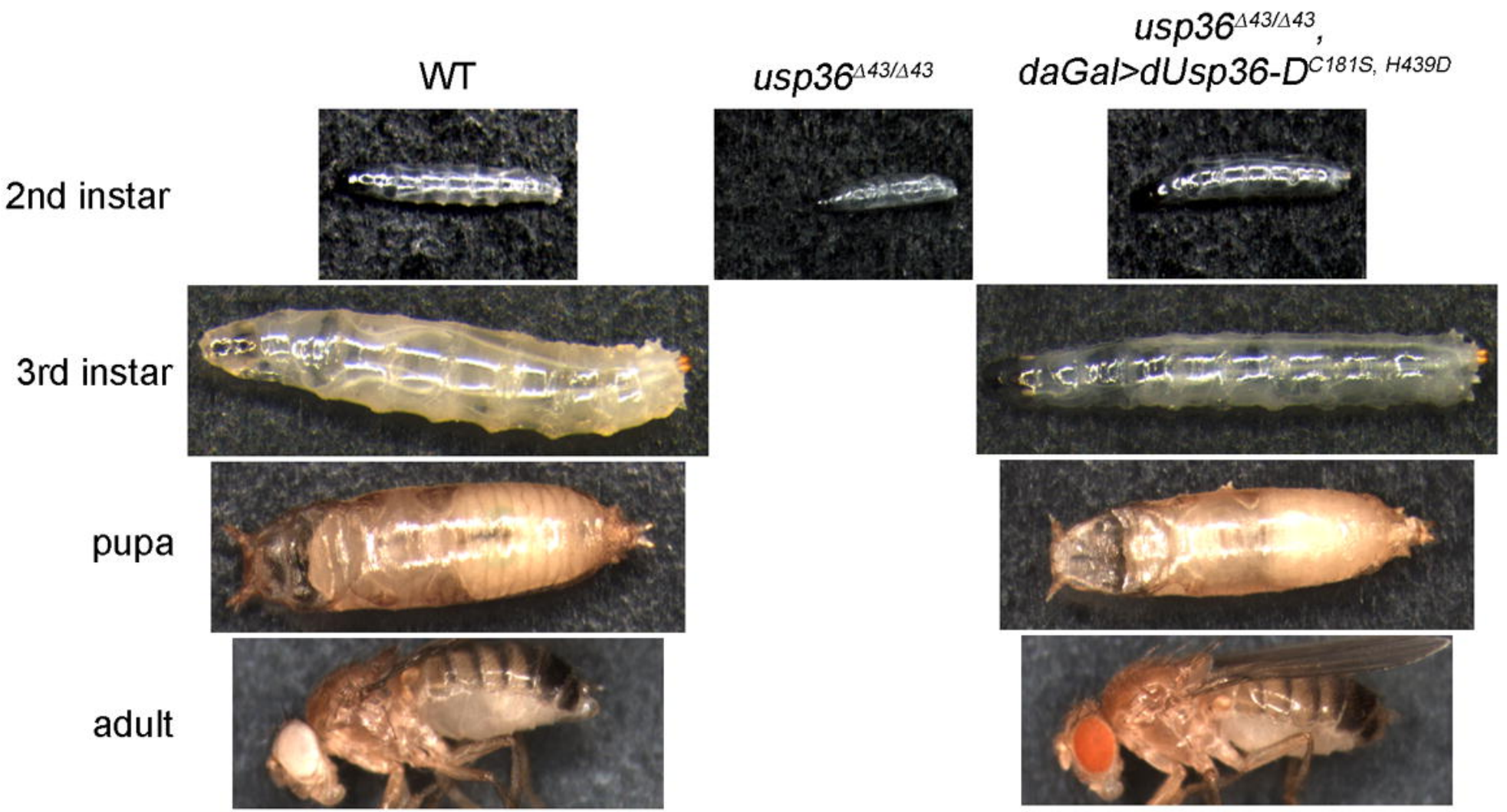
WT
usp36Δ43/Δ43
usp36Δ43/Δ43,
daGal>dUsp36-DC181S, H439D
2nd instar
3rd instar
pupa
adult

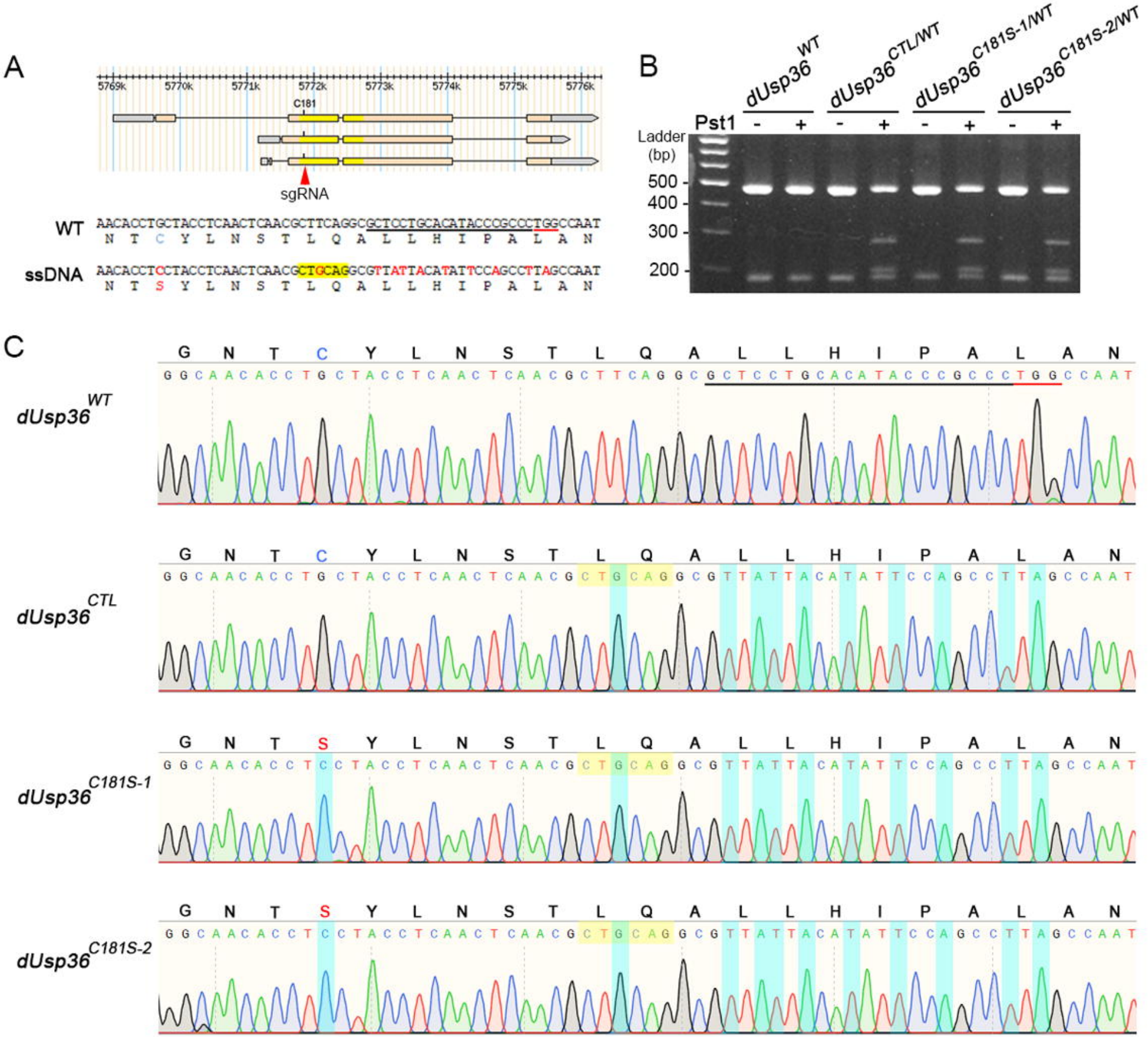
A
5769k
5770k
5771k
5772k
5773k
5774k
5775k
5776k
C181
sgRNA
WT
AACACCTGCTACCTCAACTCAACGCTTCAGGCGCTCCTGCACATACCCGCCCTGGCCAAT
N T C Y L N S T L Q A L L H I P A L A N
ssDNA
AACACCTCCTACCTCAACTCAACGCTGCAGGCGTTATTACATATTCCAGCCTTAGCCAAT
N T S Y L N S T L Q A L L H I P A L A N
B
dUsp36WT
dUsp36CTL/WT
dUsp36C181S-1/WT
dUsp36C181S-2/WT
Pst1
- + - + - + - +
Ladder (bp)
500
400
300
200
C
dUsp36WT
dUsp36CTL
dUsp36C181S-1
dUsp36C181S-2
G N T C Y L N S T L Q A L L H I P A L A N
G N T S Y L N S T L Q A L L H I P A L A N